

IAC-22,C2,5,x73845

## Advancement of Extreme Environment Additively Manufactured Alloys for Next Generation Space Propulsion Applications

Paul Gradl <sup>a\*</sup>, Omar R. Mireles <sup>a</sup>, Colton Katsarelis <sup>b</sup>, Timothy M. Smith <sup>d</sup>, Jeff Sowards <sup>b</sup>, Alison Park <sup>c</sup>, Poshou Chen <sup>b</sup>, Darren Tinker <sup>a</sup>, Christopher Protz <sup>b</sup>, Tom Teasley <sup>a</sup>, David L. Ellis <sup>d</sup>, Christopher Kantzos <sup>d</sup>

<sup>a</sup> Propulsion Department, NASA Marshall Space Flight Center, Huntsville, AL 35812, USA

<sup>b</sup> Materials and Processes Laboratory, NASA Marshall Space Flight Center, Huntsville, AL 35812, USA

<sup>c</sup> NASA Safety and Engineering Center, NASA Langley Research Center, Hampton, VA 23666, USA

<sup>d</sup> High Temperature and Smart Alloy Branch, NASA Glenn Research Center, Cleveland, OH 44135, USA

\* Corresponding Author, Paul.R.Gradl@nasa.gov

### Abstract

The National Aeronautics and Space Administration (NASA) has been involved in the development and maturation of metal additive manufacturing (AM) for space applications since the late 2000's. Several efforts focused on the understanding of AM processes through material characterization and testing, standards development, component fabrication, and infusion into propulsion development and flight applications. NASA matured commonly used aerospace alloys from various alloy families (Nickel, Copper, Stainless and Steel, Aluminum, and Titanium-based) through detailed AM process and heat treatment characterization, in addition to mechanical and thermophysical testing. While these alloys are actively used in many propulsion applications, there is a need for ongoing AM optimized alloys using integrated computational materials engineering (ICME) and process development for high performance applications. The applications targeted are liquid rocket engines; advanced propulsion systems; and in-space propulsion with high heat fluxes, high pressure, and/or that use propellants that can degrade alloys (e.g., hydrogen). This paper highlights the characterization and physical properties of the more common AM alloys using laser powder bed fusion (L-PBF) and laser powder directed energy deposition (LP-DED) processes. Additionally, this paper discusses some of the ongoing novel alloy development and maturation using AM for use in these harsh environments, such as GRCop-42, GRCop-84, NASA HR-1, GRX-810, and C-103. The results from these processes demonstrated that AM could enable rapid development and ongoing efforts for optimized alloys using ICME, yielding higher performances. These alloys have undergone modeling, fundamental metallurgical evaluations, heat treatment studies, detailed microstructure characterization, and mechanical testing campaigns. This, combined with direct application-specific component fabrication and hot-fire testing, enabled the increase of the Technology Readiness Level (TRL) through high duty-cycle testing. A background and overview of these novel AM-enabled alloys and AM processing developments including metallurgical and mechanical property studies is presented here. The latest advancement in the parallel component development and hot-fire testing and future developments for these alloys is also discussed.

**Keywords:** Additive Manufacturing, Propulsion, Rockets, Alloy Development, GRCop-42, GRCop-84, Refractory, GRX-810, NASA HR-1, L-PBF, LP-DED, DED, Laser Powder Bed Fusion, Laser Powder Directed Energy Deposition

### Acronyms/Abbreviations

AM Additive Manufacturing (AM), Carbide Dispersion Strengthened (CDS), Directed Energy Deposition (DED), Domestic or Foreign Object Debris (DOD or FOD), Hydrogen Environment Embrittlement (HEE), Hydrogen Embrittlement Index (HEI), Hot Isostatic Pressing (HIP), Integrated Computational Materials Engineering (ICME), Low Cycle Fatigue (LCF), Laser Powder Bed Fusion (LPBF), Laser Directed Energy Deposition (LP-

DED), Liquid Rocket Engine (LRE), Manufacturing Technology Demonstrator (MTD), National Aeronautics and Space Administration (NASA), Nuclear Thermal Propulsion (NTP), Oxide Dispersion Strengthened (ODS), Powder Bed Fusion (PBF), Reaction Control System (RCS), Refractory High Entropy Alloys (RHEA), Technology Readiness Level (TRL), Ultimate Tensile Strength (UTS)

## 1. Introduction

Material selection for an end use aerospace application is critical for both component and mission success. Aerospace propulsion components provide unique challenges due to the demanding end-use environments in addition to programmatic and system requirements to meet mass, economics, and acceptable risk [1]. Appropriate selection, use of metal alloys, and how they are processed throughout the entire component life cycle has a significant impact on the success of components when they are placed into service [2]. Propulsion components are typically designed with minimal margins to reduce mass, so a thorough understanding of the material behavior under the expected operating conditions and environment is critical. While various materials are used for propulsion components, metals and metal alloys are the most common. They often come from alloy families including aluminum-, stainless steel, titanium-, nickel- and iron-based superalloys, copper-, refractory-, and platinum-based alloys [3].

The metals and metal alloys used for propulsion applications must meet a long list of technical requirements in addition to satisfying programmatic goals. These requirements often include high strength-to-weight ratios, capacity to operate cyclical and sustained static and dynamic loads (i.e., long-life duty cycles), chemical compatibility with fuels and/or oxidizers, the ability to withstand both cryogenic ( $-253\text{ }^{\circ}\text{C}$ ) and elevated temperatures (often  $>1,000\text{ }^{\circ}\text{C}$ ), and to have thermal expansion coefficients equivalent to alloys to which they are mated or joined. These requirements stem from harsh operating of modern liquid rocket engines where chamber temperatures can exceed  $3300\text{ }^{\circ}\text{C}$  and where the chamber and coolant pressures exceed 410 bar. Programmatic goals that generally enforce weight minimization and associated performance requirements can result in thin walls ( $<1\text{ mm}$ ) that must withstand high heat flux. The combination of harsh chamber conditions and thin hot walls results in high thermal gradients often exceeding  $230\text{ }^{\circ}\text{C}$ , inducing high thermal stresses alone. In addition to demanding high performing tensile and fatigue properties, fracture toughness is essential due to potential impacts from domestic or foreign object debris (DOD or FOD). Depending on the environment corrosion resistance and wear resistance may also be required.

Other environmental factors such as radiation, atomic oxygen, ultraviolet, or plasma may also place additional requirements on the properties required for a material. The operating environment thus drives the desired properties for an alloy including mechanical, physical and thermophysical. These properties are derived from the interconnection between the process-microstructure-properties ultimately leading to end-use performance.

Various traditional manufacturing processes and techniques for aerospace components are well-matured and the alloys produced from these processes well-characterized to produce flight components. These processes can include forgings, castings, machining, welding, brazing, inspections, heat treatment, and other assembly operations to fabricate the final component and system. The manufacturability and sequence of operations (including supply chain and processing economics) are necessary considerations for component and system designs but can lead to long lead times and cost increases. Additionally, propulsion components are often produced in low volumes ( $<100$  units) and specialty process development can be costly if not fully amortized. While design and integration of components and system is arduous, the manufacturing stage is when most of the program problems arise. There are opportunities to improve or replace the existing manufacturing techniques to reduce costs and eliminate non-conformances. In addition to improving or replacing the manufacturing processes, there are opportunities for new alloys to enable higher performance.

Additive Manufacturing (AM) has matured rapidly for use in propulsion systems with many components in both flight and in developmental applications. AM has demonstrated schedule savings of 2-10x over traditional methods and also allows for regular and early developmental manufacturing and testing to iterate designs. Cost reduction has also been continuously demonstrated using AM for complex components on the order of 50% or greater. To achieve these gains, AM must be applied intentionally and methodically to obtain potential technical and economic advantages with strong consideration of the alloy being used. While AM has shown advantages for cost and schedule reductions, it also offers new opportunities to alloy for higher performance alloys.

**Table 1. Specialty AM alloys developed with different purposes for propulsion components.**

Max. Use Temp. (°C)	Alloy Family	Purpose	Novel AM Alloys	Propulsion Use
200	Aluminum	Light weighting	-	Various
750	Copper	High conductivity; strength at temperature	GRCop-42 GRCop-84	Combustion Chambers
800	Iron-Nickel	High strength and hydrogen resistance	NASA HR-1	Nozzles, Powerheads
900	Nickel	High strength to weight	-	Injectors, Turbines
1100	ODS Nickel	High strength at elevated temp; reduced creep	GRX-810 Alloy 718-ODS	Injectors, Turbines
1850	Refractory	Extreme temperature	C-103, C-103-CDS, Mo, W	Uncooled Chambers

AM maturation started with a limited number of commonly available alloys – Ti6Al4V, AlSi10Mg, Inconel 625, Inconel 718, CoCr, and 316L stainless steel for example [1,3]. This led designers to use what was available, but not always what provided the optimal design solution. Propulsion applications tend to be more risk-sensitive, so a design may lean towards the selection of common, accessible, and well-matured AM alloys over a new an AM alloy that needs to be developed, characterized, and matured [4]. As many AM processes have become standardized and more widely accepted, the adoption of new alloys for AM may readily occur with a greatly reduced developmental cycle per material. NASA specifically identified this need for various propulsion applications as well as the gap to develop and mature new alloys using AM processes. A specific goal in new alloy development was not only to increase the end-use alloy performance, but also ensure robust printing to eliminate issues that can arise during traditional manufacturing. Having the choice of new alloys that are intentionally enabled by AM could provide many benefits: expanded design options, improved product performance, and reduced post-processing costs. NASA has advanced AM alloys to meet end use environments under alloy families such as copper, Fe-Ni, high temperature superalloys (i.e., ODS), and refractories. Each of these alloys has different target use applications and derived specific to the requirements described previously. Alloys discussed in this paper include GRCop-42 (Cu-4 wt.% Cr-2 wt.% Nb) and GRCop-84 (Cu-8 wt.% Cr-4 wt.% Nb), NASA HR-1 (Fe-Ni-Cr), JBK-75 (Fe-Ni-Cr), GRX-810 (Ni-Co-Cr), C-103 (Nb-10wt.%, Hf-1wt.%, Ti), Tungsten (W), and Molybdenum. The use temperature and purpose of these

custom alloys is shown in Table 1. The unique category of oxide dispersion strengthened (ODS) nickels use a nanoscale oxide such as yttria (Y<sub>2</sub>O<sub>3</sub>), zirconia (ZrO<sub>2</sub>), or thoria (ThO<sub>2</sub>) for strength and creep improvements.

Several of these alloys have roots using traditional techniques but were not advanced due to challenges with production in the wrought form or economic reasons. In fact, alloys such as NASA HR-1 were developed using wrought and traditional processes then shelved for 15 years. AM has brought about rapid development with a reduced supply chain and build process schedule. This has revived interest in previously difficult-to-process alloys or new alloys only enabled by AM. The alloys described in this paper fill several gaps for materials needed in liquid rocket engine environments including hydrogen resistance, high pressure environments, extreme temperatures, creep resistance, and a combination thereof. This paper describes the importance of each of these AM alloys for propulsion, the development work completed on these including the formulation, AM build processes, characterization, heat treatment optimization, microstructure characterization, mechanical and thermophysical testing, and hot-fire testing. Proper maturation of the alloys requires a thorough understanding of the entire AM lifecycle from component conceptual design through end-use service life to successfully implement.

## 2. AM Processes and Development

### 2.1. *AM Processing Lifecycle*

The AM lifecycle is inclusive of various steps that include the design and analysis of the part and build, the

AM build processes with inputs including feedstock and build parameters, post-processing, and finally verification and certification before the part is placed into service [3]. Post-processing may include operations such as powder removal, support removal, build plate removal, heat treatments (i.e., stress relief, hot isostatic pressing (HIP), solution, aging, etc.), cleaning, inspections, machining, polishing, and joining. Since the AM process is tightly integrated through all process steps, there are many opportunities where defects can manifest or improper order of operations that can reduce performance. The manufacturing process derived for AM is much more than just printing the part. The successful development of new AM alloys integrates all the above steps.

Various AM processes have been matured to produce the NASA AM alloys for specific component applications [5]. The AM processes are categorized into melting processes and solid-state processes. Each has unique advantages and challenges, and many are supplemental to one another. The most commonly used AM processes to produce components are powder bed fusion (PBF) and directed energy deposition (DED). The PBF process, specifically laser powder bed fusion (L-PBF) manufactures parts using a bed of powder and a laser as the energy source. The laser melts the powder in a defined scanning strategy to create features within a discrete layer. The build chamber is fully purged and a recoater arm provides a new layer to be melted in a layer-by-layer operation to build a complete component. L-PBF is most often used for fine feature components but is limited in overall build volume. GRCop-42, GRCop-84, GRX-810, C-103 all made use of L-PBF since these alloys are used in components that require small feature resolution such as combustion chambers and injectors.

Another AM process used to manufacture custom NASA alloys is DED, which has several variations based on feedstock and energy source (i.e., laser, electron beam, electrical arc). The most common DED method is laser powder directed energy deposition (LP-DED) providing medium resolution features, but exceptionally large build volumes. LP-DED uses a deposition head with off-axis or coaxial nozzles that blows powder into a melt pool created by a laser. This deposition head is attached to a gantry or robotic motion control and defined toolpath from the part CAD geometry. A local purge or fully inert build chamber is used to reduce oxygen and a trunnion table is typical of the motion control system allowing for multiple axis orientations for part deposition. The hydrogen-resistant NASA HR-1 and JBK-75 alloys were targeted for use with the LP-DED allowing for large scale integral channel wall nozzles to be built. GRCop-42 and C-103 have also been built using the LP-DED process

and plans are in place for GRX-810 LP-DED development.

AM build process selection is critical for parts to be built successfully and for fully realizing economic benefits offered by AM. This was previously discussed in a detailed paper [3]. Attributes that can discriminate between the processes include overall part size, part complexity, feature resolution, process economics and availability, industrial maturity, post-processing, and metallurgical characteristics and properties. A typical input prior to process selection is the type of alloy. Each AM process has unique attributes and not all the novel alloys can be built using all the processes. Feedstock is an important discriminator here. The alloys defined in this paper are readily available as a powder feedstock and are the most economical source for AM processes. GRCop-42 and GRCop-84 require gas atomization using argon to form the chromium-niobium in suspension for the dispersion strengthening [6]. NASA HR-1 and JBK-75 are produced using rotary atomization but can be produced using gas atomization [7]. C-103 and GRX-810 also use gas atomization. GRX-810, ODS, and carbide dispersion strengthened (CDS) family of alloys all require a coating process for the powder following atomization [8].

## 2.2. ICME Modeling for Novel Alloys

Integrated Computational Materials Engineering (ICME) is a transformative discipline that enables rapid materials development through computational methods that integrate materials information with processing and performance [9]. Infusion of ICME into AM workflows provides numerous benefits such as rapid maturation of AM processes from the initial formulation through development to production of flight-certified parts [10]. ICME approaches are now being adopted widely (beyond as an academic tool) due to the reduction in the material maturation cycle. NASA is using such approaches to develop new alloys with optimal 3D printing characteristics including printability of new refractory alloys and enhanced mechanical performance of oxide dispersion strengthened nickel-based alloys. Two examples on the usage of ICME at NASA centers for the development of such materials is described here.

A first example of ICME implementation at NASA is the circumvention of difficulty and expense associated with conventional refractory metal manufacturing methods. Under conventional manufacturing methodologies, refractory metal and alloy bar, plate, tube, and sheet are fabricated through various forming and joining cycles leading to difficulties with machining a hard material, difficulty in producing defect-free joints,

and high expense and material waste of value-added stocks. Additive manufacturing can mitigate much of the waste and expense but requires refractory metal and alloy feedstocks that are printable (resistant to formation of build defects). There is opportunity to reexamine the refractory metal alloy space using computational approaches combined with limited empirical validation to develop new printable alloys in the W, Nb, Mo, and Ta families.

Several metallurgical issues arise during printing of such materials: 1) solidification cracks occur during terminal stages of alloy solidification, 2) large grain formation due to epitaxial growth and thermally activated grain growth, and 3) a shift in ductile-to-brittle behavior at greater-than-ambient temperature resulting in cracks as the grain size increases. The approach to mitigate these issues is through inoculation of powder feedstocks with high melting point intermetallic particles (examples include ZrC, TaC, HfC), which are optimized in size and distribution to pin grain boundaries thereby preventing grain growth and associated embrittlement. Addition of these particles alters the solidification behavior and can unfortunately promote solidification cracking during the build. ICME tools (including CALPHAD and custom Python routines for solidification crack modeling and particle coarsening) are used to find regions of optimal powder addition where grain growth and solidification cracking are both minimized. Figure 1 shows an example of hundreds of solidification cracking and particle coarsening simulations of the W-Zr-C ternary system, mapping out regions of cracking susceptibility. Darker contours suggest compositions where a new alloy would be most crack-resistant and lighter contours suggest compositions expected to be most crack susceptible. To map this space empirically would require hundreds of powders to be formulated and printed which is unequivocally cost prohibitive. Yet with ICME, the composition space can be mapped on a workstation in less than 24 hours, and then validate computed findings empirically with a few select data points to guide production of future W and W-alloy powders using the inoculant addition approach.

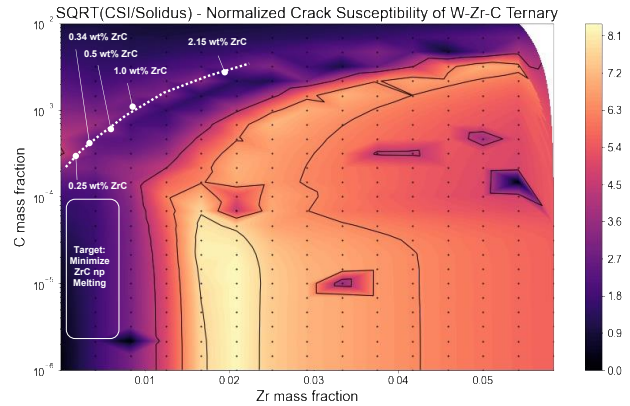


**Figure 1. Calculated solidification cracking susceptibility of the W-Zr-C ternary system. Dark contours represent regions of lowest cracking susceptibility.**

A second example involves early promising results from NiCoCr-ODS alloy production using L-PBF at the NASA [8]. CALPHAD modeling was employed to produce a new ODS composition utilizing the equiatomic NiCoCr system as the foundational base chemistry. From these simulations a few notable findings were made. It was evident that Mo additions typically stabilized unwanted phases (e.g.,  $\sigma$ ,  $\mu$ ) and the ratio of Ti to Nb was critical for the stabilization of MC carbides especially at 1093°C. Previous ODS alloys developed for AM indicated that grain boundary oxidation played a significant role ultimate tensile strength and ductility variations. In turn, MC carbides were targeted to improve grain boundary strengthening and oxidation resistance [11]. The solid solution strengthening was targeted for improvement from existing Ni-based alloys while maintaining phase stability up to and at the target test temperature of 1093°C. The freezing range was targeted to remain under 100°C. Certain elements had unexpectedly large impacts on the freezing range and were assumed as unwanted additions for an alloy designed for printability. Over 50 simulations were completed to keep these different factors in balance. Unwanted phases, namely  $\sigma$  and  $\mu$ , were effectively suppressed as low as 810°C, hence the alloy was named GRX-810. The simulations suggested this new composition had the best balance between printability, strength, oxidation resistance, and phase/microstructure stability. The new composition was termed GRX-810 with intention to balance printability, strength, oxidation resistance, and phase/microstructure stability. Figure 2 reveals the amount of each phase in the temperature range 800-1500°C, as predicted by the thermodynamic model for GRX-810.

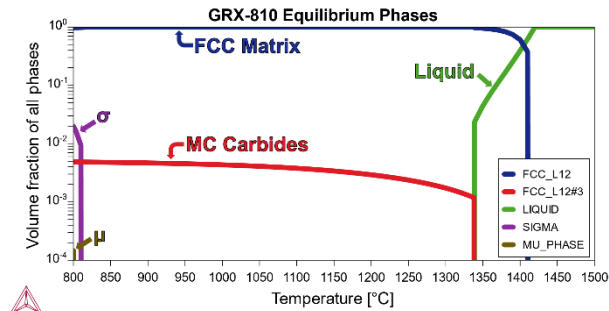


**Figure 2. Predicted phase stability of GRX-810 between 800-1500° C. No detrimental phase formation is predicted to be stable above 810° C.**

Both examples above provide a snapshot of hundreds of virtual experiments that were enabled by ICME approaches. There is no need to create hundreds of new powder lots, fabricate thousands of samples, and then perform extensive material evaluations. Instead, off-the-shelf and custom codes may be used to rapidly screen large composition spaces with a desired performance metric and optimize chemistry. Such techniques are being slowly adopted for propulsion applications. There is still tremendous opportunity yet available to infuse ICME into development cycles for next generation space propulsion alloys.

### 3. Maturation of Alloys for Propulsion

#### 3.1. Alloy Selection for Propulsion Components

Each component in a liquid rocket engine system must complete a methodical trade to determine the appropriate alloy requirements based on the environment, system loads, and life requirements. Combustion chambers operate at high heat fluxes from the combustion products and are most often actively cooled using the propellants (most often fuel) to maintain reasonable wall temperatures and avoid melting [12]. Copper-alloys are often used due to the high conductivity and strength at wall temperatures that can exceed 750 °C [13]. Low cycle fatigue (LCF) is often a key consideration as chambers must survive multiple starts and sustained duty cycles for reusability. Due to the environment from the propellants, oxidation can lead to blanching, and hydrogen can cause hydrogen environment embrittlement [14]. NASA has matured GRCop-42 and GRCop-84 to meet these requirements. The GRCop-alloys (i.e., Glenn Research Center Copper) were developed as a high strength and high conductivity alternative to other commonly used copper-alloys such as C-18150 (Cu–1.5 wt.% Cr–0.2 wt.% Zr), NARloy-Z (Cu-3 wt.% Ag-0.5 wt.% Zr),

Glidcop-15 (Cu-0.15 wt.% Al), and C-18200 (Cu–1.2 wt.% Cr).

A general comparison of the copper-alloys is shown in Figure 3 comparing conductivity with yield strength at room temperature (22 °C). A single plot is often difficult to capture the entire material trade since only two of the criteria are shown and can also change at elevated temperatures or different conditions. For instance, pure copper is limited to approximately 200°C before it reaches a significant reduction in strength. Other copper alloys such as C-18150 and C-18200 are generally limited to nominal temperatures of around 540 °C due to reduced strength or changes in properties due to the sustained temperatures.

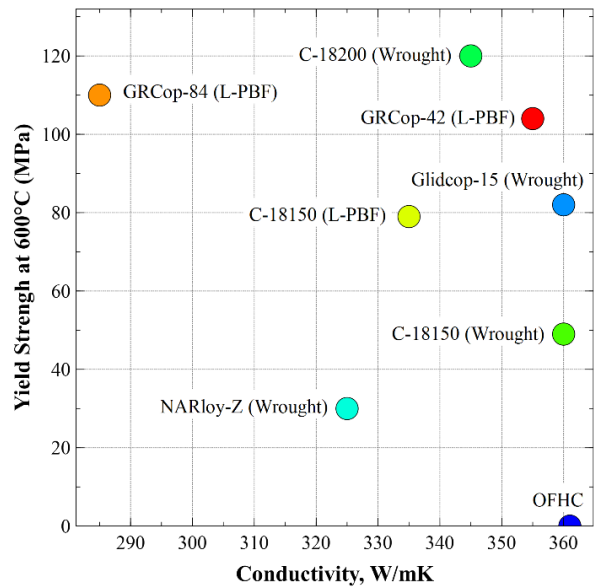


**Figure 3. Comparison plot of copper-alloy selection based on conductivity and yield strength at 600°C. Data compiled from [15–17].**

Another key component in a liquid rocket engine is the exhaust nozzle, which is typically regeneratively-cooled (regen) due to the high heat flux. The joint between the chamber and nozzle is appropriately selected to balance the heat flux with minimizing overall system weight. While the chamber uses copper-alloys for high conductivity, the regen nozzle is made from higher strength to weight alloy, typically a stainless or superalloy. The NASA HR-1 was specifically developed for regen nozzle applications using hydrogen as a propellant, allowing for resistance which otherwise causes hydrogen environment embrittlement (HEE) issues. The NASA HR-1 for AM applications was also specifically formulated for high ultimate strength in this environment in addition to high yield and subsequent

elongation. LCF is also a strong consideration in the nozzle design since it is tested and flown for multiple starts and missions. The conductivity was also improved in the LP-DED version of the alloy compared to the wrought version to aid with the design for nozzles.

A comparison plot is shown in Figure 4 for various superalloys, stainless steel alloys and NASA HR-1 with the hydrogen embrittlement index (HEI) along with the ultimate strength at elevated temperature. While almost no alloys are perfectly resistant to hydrogen, this plot shows an acceptable range of about 20% with a higher HEI meaning that the alloy is more prone to embrittlement. The NASA HR-1 shows a very low HEI along with a high ultimate tensile strength (UTS) at 600°C. This is a typical operating range for NASA HR-1 for regen nozzles but can exceed this temperature as well based on the environment and requirement. Other alloys such as 316L can meet the HEI requirement, but with a significant reduction in strength. Superalloys such as Alloy 625 (Inconel 625) and Alloy 718 (Inconel 718) can be used in this environment but will require a significant reduction in material properties to account for the HEE.

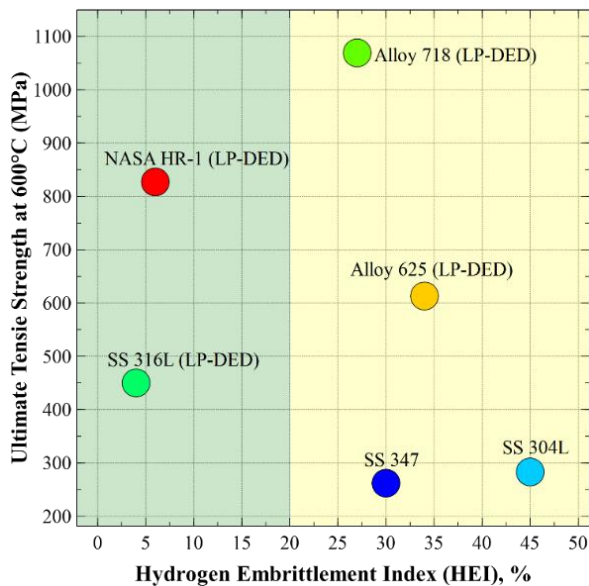


**Figure 4. Comparison plot of NASA HR-1, superalloys, and stainless alloys comparing the hydrogen embrittlement index (higher HEI = more susceptible) to ultimate strength at 600 °C.**

The NASA HR-1 offers an excellent balance of the high strength, HEE resistance, LCF, thermal conductivity and ductility to meet the channel-cooled nozzle and other component designs used in hydrogen or other propellants.

Propulsion components such as rocket injectors, nozzles, turbines blades, combustors, and other hot section components operate at elevated temperatures for sustained durations and high duty cycles. Typically Ni-based superalloys are used in these environments but are generally limited to 900 °C or less in many cases for sustained temperatures. While Ni-alloys can operate in temperatures up to 1200 °C, this is not a realistic design temperature for this type of material. This can limit the overall performance of these components and the overall system may not be optimized due to temperature limits in a turbine or injector faceplate. Other challenges with current components include creep rupture, which is a necessary design consideration for sustained durations and high duty cycles such as those for aircraft engines. The GRX-810 (i.e., Glenn Research Center Extreme) alloy was developed and is being further matured to allow an increase in operation temperatures for these various components. The alloy is Ni-Co-Cr and incorporates oxide dispersion strengthened (ODS) coating of the powder to allow the high performance at elevated temperature. Traditionally manufactured ODS alloys were plagued with high expenses due to the manufacturing process, but AM is enabling more economical high performance ODS alloys, like GRX-810, to be produced.

While operating temperatures and creep are a couple of considerations, the mechanical properties such as ultimate and yield as well as physical properties such as density need to be considered for optimal designs. The GRX-810 alloy compared to other superalloys and ODS superalloys is shown in Figure 5. For reference the AM Ni-Co-Cr using L-PBF is also shown on the same graph and is without ODS. The strength of the GRX-810 with the ODS nearly doubles the strength at temperature. An additional advantage of ODS alloys includes improved oxidation properties at elevated temperatures by promoting and stabilizing Alumina or Chromia oxide scale formation. The creep rupture life of GRX-810 is orders of magnitude improvement over some of the more traditional Ni-based superalloys such as Alloy 625 and Alloy 718.

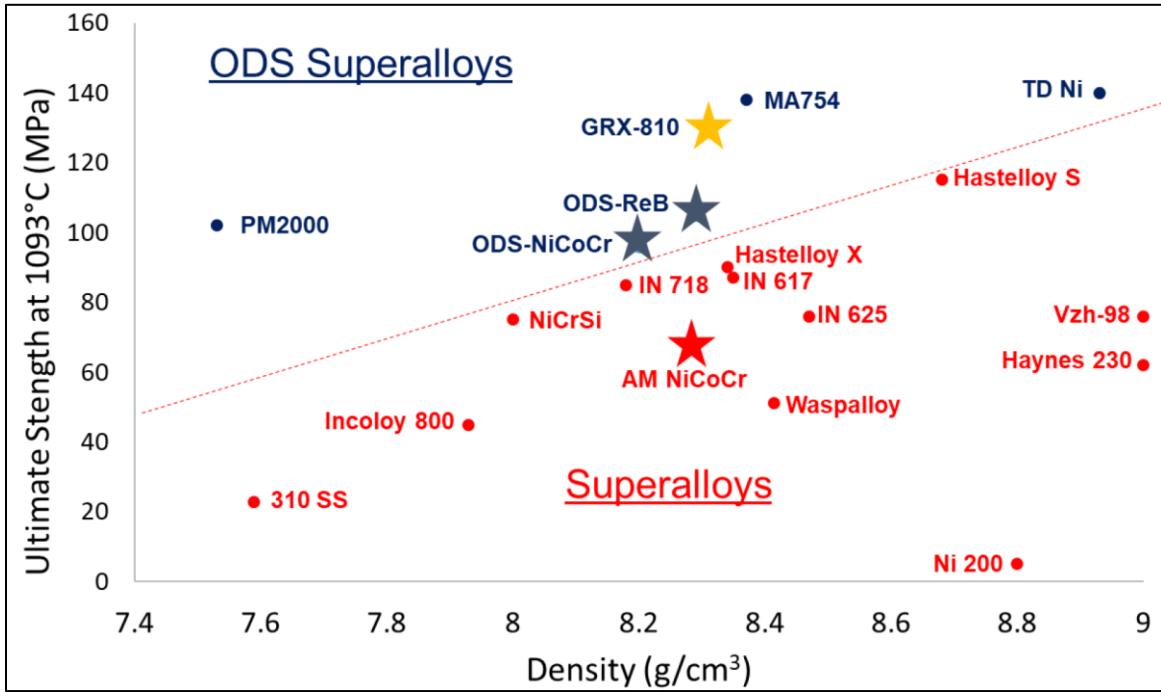


Figure 5. Comparison of ultimate tensile strength at elevated temperature (1093°C) with density for GRX-810 and other ODS alloys as well as Ni-based superalloys.

Refractory metals such as Niobium (Nb), Molybdenum (Mo), Tantalum (Ta), Rhenium (Re), and Tungsten (W) and their alloys are used for extreme high temperature environment service. Refractory metals are desirable due to a high melt temperature ( $T_m$ ) and the ability to retain strength and hardness at elevated temperatures but in most cases have a higher density than Ni-base superalloys [18]. Examples of applications include in-space radiatively cooled thrusters, reaction control system (RCS) thrusters, nuclear thermal propulsion (NTP) fuel and structure, hypergolic and green propulsion chambers, nuclear power system in-core heat pipes and heat exchangers, electric propulsion, aeroengine turbines, hypersonic wing leading edges, and plasma facing components in fusion reactors. Refractory metals and alloys extend the operating temperature to between 1100-2500 °C depending on the selected material, as shown in the red bullets in Figure 6. Selection of a specific metal or alloy is highly dependent on expected operating conditions to include temperature, environmental exposure (i.e. oxidizing, reducing, inert, vacuum), desired mechanical properties, neutron absorption cross-sections, etc.

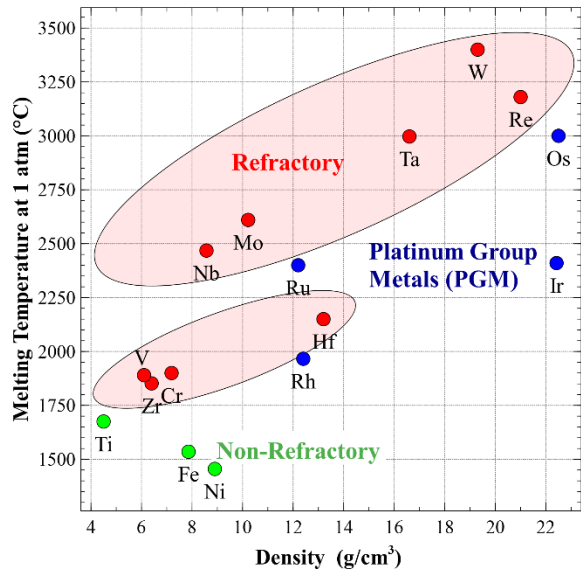


Figure 6. Refractory elemental density compared to melting point at 1 atm.

#### 4. High Conductivity GRCo-42 and GRCo-84

The GRCo-alloys are dispersion strengthened through Cr<sub>2</sub>Nb precipitates established during the powder atomization and further enhanced during L-PBF processing. The GRCo-alloys were specifically formulated to allow for high strength at temperature, hydrogen environment resistance, high conductivity and extended low-cycle fatigue (LCF) properties. The formulation for GRCo-42 and GRCo-84 is shown in Table 2. The GRCo-alloys also allow improved oxidation and blanching resistance with thermal and oxidation-reduction cycling, allowing for high duty cycles. Hot wall temperatures in combustion chambers can exceed 750°C for sustained durations using the GRCo-alloys, depending on the strength and creep requirements.

**Table 2. Chemistry of GRCo-42 and GRCo-84.**

Element	GRCo-42 wt. %	GRCo-84 wt. %
Cu	Balance	Balance
Cr	3.1 – 3.4	6.2 – 6.8
Nb	2.7 – 3.0	5.4 – 6.0
Fe	Target <50 ppm	Target <50 ppm
O	Target <250 ppm	Target <250 ppm
Al	Target <100 ppm	Target <100 ppm
Si	Target <100 ppm	Target <100 ppm
Cr:Nb Ratio, wt. %	1.13 – 1.18	1.13 – 1.18

In 2014 NASA started development of the GRCo-84 alloy using the L-PBF process and successfully printed and hot-fire tested various chambers. Material characterization and property development was also performed. While the GRCo-84 allows for high strength and good LCF properties, there was a desire to improve the thermal conductivity. NASA started development of GRCo-42 in 2018 to mature the alloy through development of material properties, component demonstrations, and hot-fire testing. A critical task in developing these alloys were the establishment of the powder supply chain and commercial print services to permit accessibility of the GRCo-alloys for commercial space use. As of 2022, more than seven U.S. vendors are actively producing

the GRCo powder and more than 10 commercial print services providing this as a standard material option.

An extensive effort was established to develop properties related to the GRCo-alloys and to make these accessible to industry. Due to the dispersion strengthening, the GRCo-alloys do not require heat treatment. Only a HIP is required to achieve full mechanical and thermophysical properties. The typical average tensile curve for GRCo-42 and GRCo-84 is shown in Figure 7. An advantage of the GRCo-alloys are high conductivity and strength at the elevated temperatures and stability during operation. The GRCo-84 has demonstrated higher strength at various temperatures due to the higher content of Cr:Nb and improved low cycle fatigue properties. An advantage of the GRCo-42 alloy is the improved conductivity of about 20-30% over GRCo-84 as shown in Figure 8.

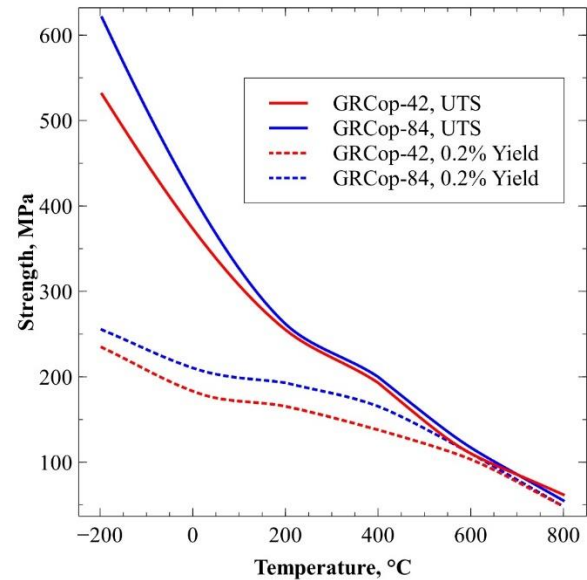


**Figure 7. Typical average ultimate tensile and yield strength vs. temperature for GRCo-42 and GRCo-84 alloys.**

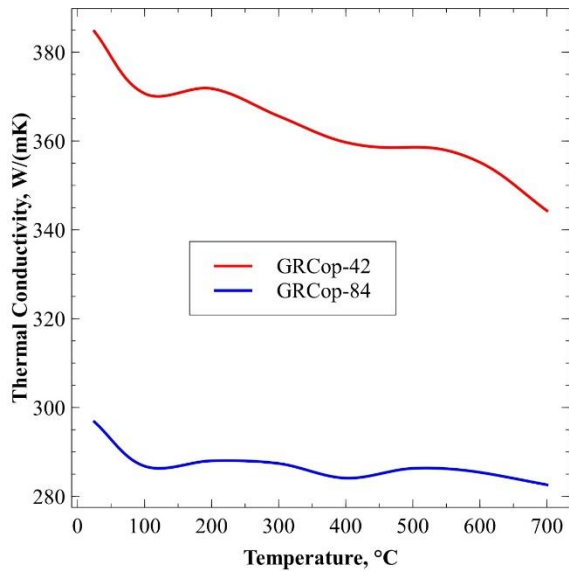


**Figure 8. Average conductivity vs. temperature for GRCop-42 and GRCop-84.**

NASA has utilized GRCop-alloys in the manufacturing and testing of over 62 combustion device components and several more in commercial space applications. These include chambers, injectors, and ignition systems using L-PBF. Additional development work has been completed using the LP-DED process, but no components have been tested using this process as of this publication. Many of the chambers produced have been successfully hot fire validated at over 1,000 starts and greater than 41,000 seconds of cumulative duration to date. A single GRCop-42 L-PBF chamber was successfully tested over 10,000 seconds and 293 starts and a second chamber over 7,400 seconds and over 168 starts. These statistics demonstrate the robustness and versatility of the GRCop-alloys. No damage to the chambers from blanching, cracks, or other issues commonly observed was seen. NASA has completed testing in Liquid Oxygen/Hydrogen (LOX/H<sub>2</sub>), LOX/Kerosene (LOX/RP-1), and LOX/Methane (LOX/CH<sub>4</sub>) using various GRCop-42 and GRCop-84 chambers. Examples of hot-fire testing and development chamber units are shown in Figure 9.

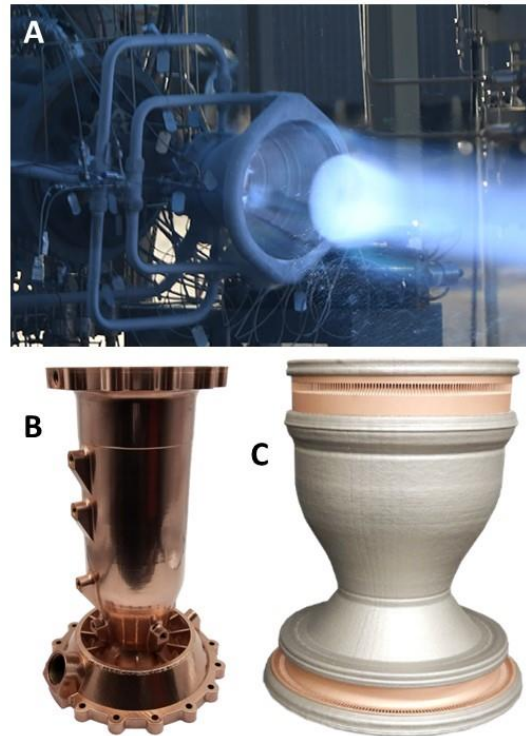


**Figure 9. Development and hot-fire testing of GRCop-alloy chambers. A) Hot-fire testing of a 31 kN LOX/CH<sub>4</sub> lander GRCop-42 chamber for 51 cycles, B) Polished GRCop-42 chamber, C) Bimetallic chamber using L-PBF GRCop-42 liner and NASA HR-1 LP-DED jacket.**

Furthermore, the potential for rocket propulsion applications using GRCop-alloy has been found to be extensive. AM of GRCop-alloys allows for custom and complex designs to balance heat transfer and friction factors (pressure drop). Customization of surface finish texture and porosity in the L-PBF process allow engineers a broader trade space for liquid rocket engine design. High porosity allows for the production of transpiration features for active cooling of components such as an injector faceplate. Surface finish enhancements allow for the reduction of pressure losses and customization of desired engine heat load which impacts downstream component performances such as injector combustion efficiency via coolant exit temperature and turbopump power requirements. Lastly, while oxygen compatibility of GRCop-alloys has not been quantified, observations from hot fire testing suggests high tolerance to oxygen rich combustion environments.

Additional development using GRCop-alloys has been demonstrated with bimetallic AM. This has allowed for the high conductivity and high strength

GRCop liner and a higher strength to weight alloy, such as Alloy 625 of NASA HR-1 to be used as a structural jacket. Additional development under the NASA's Rapid Analysis and Manufacturing Propulsion Technology (RAMPT) project using axial bimetallic methods with GRCop-42 have enabled larger thrust chamber assemblies with multiple alloys and elimination of a bolted joint between the chamber and nozzle. NASA has been successful in utilizing GRCop-alloys in the design, production, and testing of calorimetry chambers. These chambers have successfully yielded heat flux profiles for constant pressure and rotating detonative combustion devices and provided the properties to enable these high heat flux applications. The versatility of GRCop-alloys is substantial, and an investment NASA will continue exploring. The powder production process and L-PBF process parameters have been fully commercialized and are in use across the propulsion industry; the most accessible alloy being GRCop-42 across the supply chain. Development has also started using LP-DED to build parts with infrared and green lasers. An example of a GRCop-42 LP-DED manufacturing technology demonstrator chamber is shown in Figure 10 using a green laser.



**Figure 10. Manufacturing demonstrator chamber using LP-DED green laser and GRCop-42.**  
[Courtesy: RPMI / TRUMPF / NASA].

## 5. Hydrogen Resistant NASA HR-1

NASA HR-1 is a high strength Fe-Ni based  $\gamma'$ -strengthened superalloy designed to resist high pressure hydrogen environment embrittlement (HEE), oxidation, and corrosion [2]. NASA HR-1 was originally derived from JBK-75 for increased strength and ductility in high-pressure hydrogen environments to meet the requirements of liquid rocket engine (LRE) applications. These requirements include yield strength, thermal conductivity, HEE resistance, ductility, and LCF. To achieve this, the chemical

composition of NASA HR-1 increased  $\gamma'$  forming elements (Ti and Al), added W and Co, and adjusted the Fe and Ni content [19]. Wrought NASA HR-1 requires costly and tedious processing that was not economically feasible for LRE components, however powder AM processes, such as LP-DED, have enabled NASA HR-1 to be a more affordable alloy for LRE applications. While adapting NASA HR-1 to the LP-DED process, it was discovered that the LP-DED process promotes Ti segregation and formation of detrimental  $\eta$ -phase more than the conventional wrought process [20,21]. As a result, the composition of NASA HR-1 was modified to the final AM revision shown in Table 3. The changes made were expected to moderately decrease strength of the LP-DED alloy while improving the ductility, LCF life, and HEE resistance from the initial composition tested in LP-DED [22].

**Table 3. Nominal chemical composition for AM NASA HR-1**

Element	NASA HR-1 Rev 3 wt.% Range	NASA HR-1 Rev 3 wt.% Target
Fe	BAL	41.2
Ni	33.7 – 34.3	34
Cr	14.3 – 14.9	14.6
Mo	1.6 – 2.0	1.8
V	0.28 – 0.32	0.3
W	1.4 – 1.8	1.6
Co	3.6 – 4.0	3.8
Ti	2.2 – 2.6	2.4
Al	0.23 – 0.27	0.25

Significant development of heat treatments and material characterization for LP-DED NASA HR-1 began in 2019 to understand and optimize the microstructure of LP-DED NASA HR-1 [3]. However, upon discovery of the Ti segregation and  $\eta$ -phase problems, the subsequent powder composition adjustments also required further adjustments to heat treatments to mitigate  $\eta$ -phase as it can severely impact the HEE resistance of NASA HR-1 [4]. Changes to the stress relief, homogenization, and solution treatment helped to minimize Ti segregation due to the LP-DED process, and the aging cycle was changed from a 1-step to a 2-step age at as this was observed to mitigate  $\eta$ -phase while minimizing the yield strength drop and improving ductility [5].

Once the heat treatments were determined, efforts focused on characterizing the mechanical and

thermophysical properties of NASA HR-1. Tensile and low cycle fatigue have been tested across a range of temperatures and testing is being performed in pressurized gaseous Hydrogen (GH<sub>2</sub>) environments to assess the HEE resistance of LP-DED NASA HR-1. The ultimate tensile strength of various LP-DED alloys compared to NASA HR-1 is shown in Figure 11. Using either the 1-step age for higher strength or the 2-step age for more ductility, NASA HR-1 performs between alloys 718 and 625. Compared to wrought NASA HR-1, LP-DED NASA HR-1 has lower strengths but higher ductility showing one of many differences between wrought and AM materials [5] Additionally, LCF testing has shown that LP-DED NASA HR-1 performs well across temperatures ranging from -196°C to 760°C (Figure 12) and has similar to slightly lower LCF life at room temperature compared to wrought in gaseous Helium (GHe) depending on the heat treatment [5], [6] These differences in mechanical properties can be attributed to compositional and microstructural differences between the wrought and LP-DED material. Thermal conductivity is another key property that was tested for LP-DED NASA HR-1 and results are shown in Figure 13 compared to other LP-DED alloys. The conductivity generally fits between stainless steel 316L and alloy 625, and LP-DED conductivity is an improvement over the data previously reported for wrought NASA HR-1 [5].

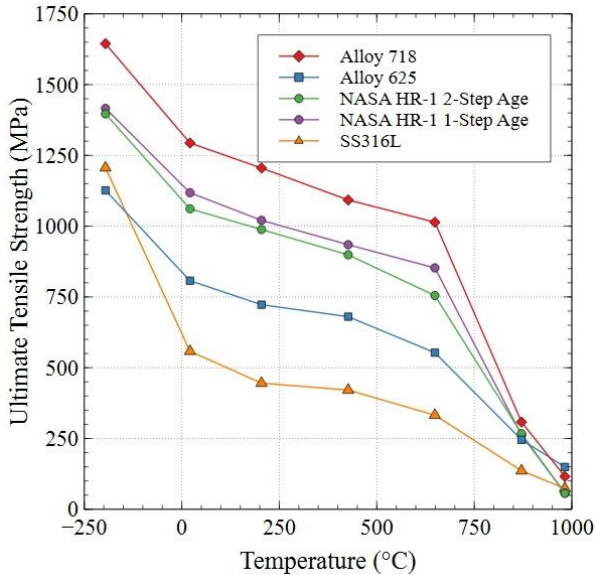


**Figure 11. Average ultimate tensile strength of LP-DED alloys versus temperature.**

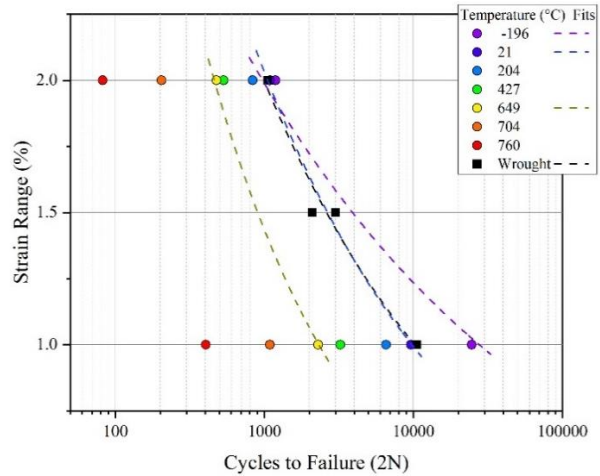


**Figure 12. Average LCF life of 2-Step aged LP-DED NASA HR-1 with changes in temperature compared to wrought values in GHe from [2], [6]**

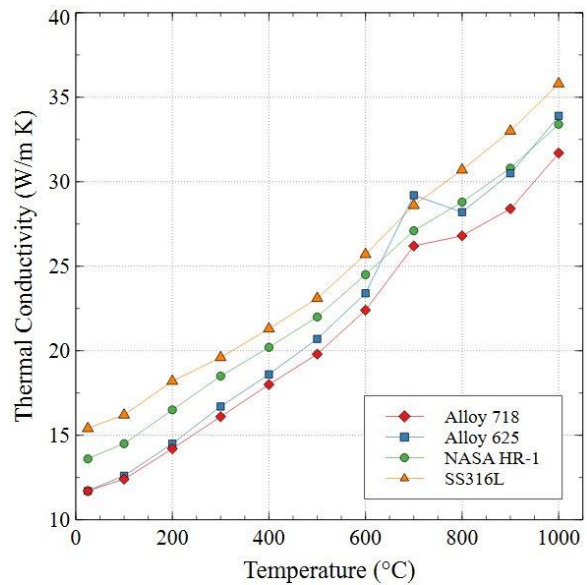


**Figure 13. Thermal conductivity of LP-DED NASA HR-1 and other LP-DED alloys vs temperature.**

NASA HR-1 alloy has been demonstrated for various combustion device components targeting channel wall nozzles. The LP-DED process has demonstrated robustness to produce large structures with integral coolant channels as well as thicker wall components for forging and casting replacements. Various parameters and corresponding laser melt can be varied to allow for different features. The lower power allows for thin walls deposited at approximately 1 mm generally used for channel wall nozzles. The higher power increases the deposition rates for thicker

wall components that are often final machined and have limited internal features. The components demonstrated include powerhead half shells (i.e., for the RS-25 Engine's powerhead), manifolds for nozzles and chambers, transfer tubes, domes, and other pressure loaded components that are used in hydrogen environments. The LP-DED process was also used to build a manufacturing technology demonstrator (MTD) at 1.52 m diameter and 1.78 m height, approximately a 65% scale RS-25 channel wall nozzle (Figure 14).



**Figure 14. 65% scale RS-25 integral channel LP-DED nozzle using NASA HR-1 (1.52 m dia. x 1.78 m height).**

NASA has completed several test campaigns to demonstrate nozzles manufactured using the NASA HR-1 alloy with the LP-DED process. Testing of a 31 kN nozzle under NASA's Long-Life Additive Manufacturing Assembly (LLAMA) project demonstrated 40 starts and 568 seconds in a LOX/CH<sub>4</sub> environment (Figure 15A). The chamber pressure of this assembly was 52 bar and mixture ratio of about 3.2. Another test campaign using LOX/GH<sub>2</sub> demonstrated high duty cycle hot-fire testing of a single NASA HR-1 LP-DED nozzle at 8.9 kN thrust and achieved 207 starts and just under 6,800 seconds. This demonstrated temperatures exceeding 760 °C on the nozzle hot wall with a chamber pressure over 76 bar and mixture ratios up to 7.5 using LOX/GH<sub>2</sub> propellants. Additional NASA HR-1 LP-DED units were tested under this campaign with unique design

features including a scalloped hot wall (tube-like) and spiral channels. All units performed as intended and met performance predictions. Two additional NASA HR-1 LP-DED channel wall nozzle units completed manufacturing and planned for LOX/LH<sub>2</sub> testing at the 156 kN thrust level. These units included a spiraled channel design and incorporated NASA HR-1 LP-DED manifolds. The deposition time for the nozzles were approximately 14 days and the manifolds were about 3 days each. NASA has manufactured multiple components using LP-DED NASA HR-1 and successfully tested components accumulating over 280 starts and 8,914 seconds in hydrogen environments on integral channel wall nozzles (Figure 15B).

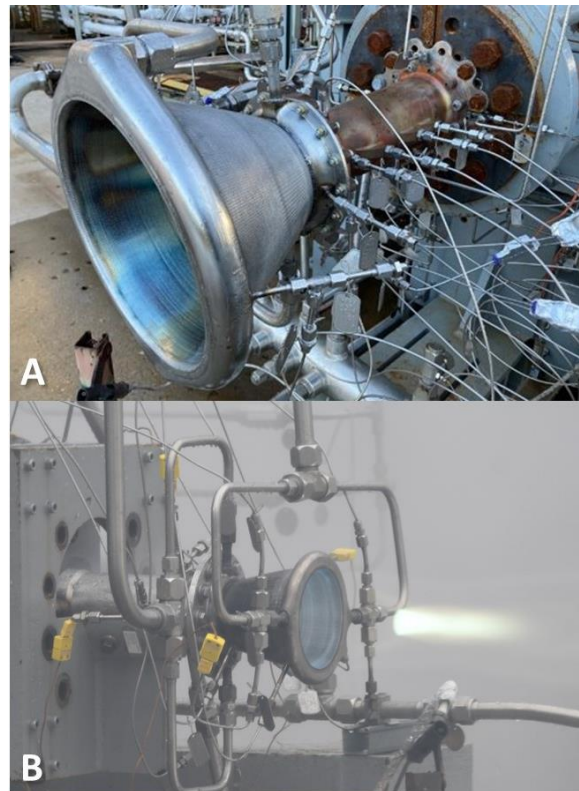


**Figure 15. NASA HR-1 nozzle test units. A) 31 kN integral channel LP-DED nozzle tested in LOX/methane, B) Hot-fire in LOX/hydrogen testing of 8.9 kN nozzle that accumulated 207 starts and 6,800 sec.**

## 6. High Temperature Superalloy GRX-810

GRX-810 is a NiCoCr-based ODS alloy specifically developed for AM. The equiatomic NiCoCr system has been shown to be quite amenable to AM [23–25]. This has been attributed to the alloys

narrow melting/freezing temperature range, the difference between the solidus and liquidus [26]. These studies have reported that the alloy maintains a solid solution in both the as-built and heat-treated conditions [25,26]. In addition, the AM-produced NiCoCr alloy provides exceptional ductility and strain hardening, comparable to its wrought counterparts. In order to further improve the high temperature properties of the NiCoCr alloy, a coating process for the AM powder feedstock was matured to produce oxide dispersion strengthened components as described by Smith et al. [26]. From this work, three different alloys were explored with the composition shown in Table 4. Notably, out of the three compositions, GRX-810 provided magnitudes of order better creep strength compared to the NiCoCr-ODS and ReB-ODS [27].

**Table 4. Compositions of ODS alloys explored and developed at NASA.**

Element	Alloy		
	NiCoCr-ODS	ReB-ODS	GRX-810
Ni	BAL.	BAL.	BAL.
Co	32	32	33
Cr	30	30	29
Re	-	1.5	1.5
Al	-	-	0.3
Ti	-	-	0.25
Nb	-	-	0.75
W	-	-	3
C	-	-	0.05
B	-	0.003	-

To produce ODS GRX-810 components. Pre-alloyed base powder with the above composition is coated with 1 wt.%  $Y_2O_3$  nanoparticles. Through Laser Powder Bed (L-PBF) AM print parameter optimization, these oxides are randomly and evenly dispersed throughout the microstructure as can be seen below in Figure 16.

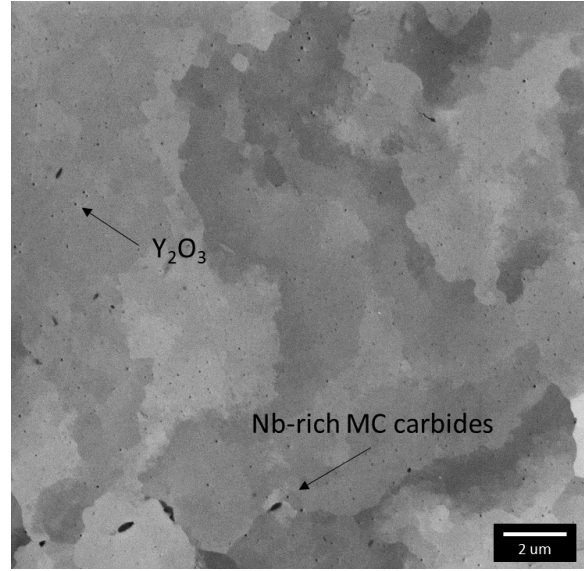


**Figure 16. A scanning electron micrograph of HIPed GRX-810 revealing a solid solution matrix with grain boundary Nb-rich MC carbides and dispersed nanoscale  $Y_2O_3$  particles.**

Scanning electron microscopy images of HIPed GRX-810 reveals a solid solution microstructure with Nb and Ti-rich MC carbides along grain boundaries. Nanoscale  $Y_2O_3$  particles can also be observed, though the resolution of this imaging technique cannot provide quantifiable characterization. Notably, no bulk oxide or slag formation was observed in these samples. From the micrograph in Figure 16 it is apparent that the as-built grain structure is retained even after a high temperature / high stress HIP cycle. This provides evidence that the oxides are well distributed and can maintain and stabilize the microstructure at much higher temperatures as compared to non-ODS alloys. Though early in the alloys development phase, it presents promising mechanical results compared to the previous NiCoCr-ODS alloys as well as conventional superalloys. The tensile and yield strengths for HIPed GRX-810 were tested from cryogenic temperatures up to 1093 °C. Test results are shown below in Figure 17 (full data in Appendix, Table A).

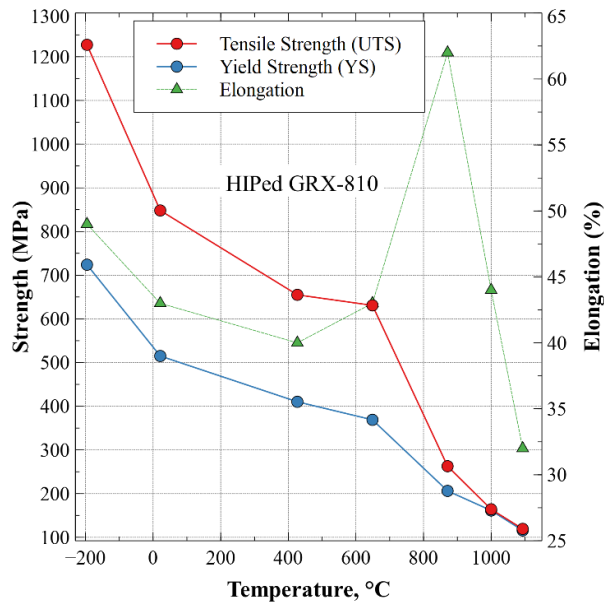


**Figure 17. The tensile properties of HIPed GRX-810 as a function of temperature.**

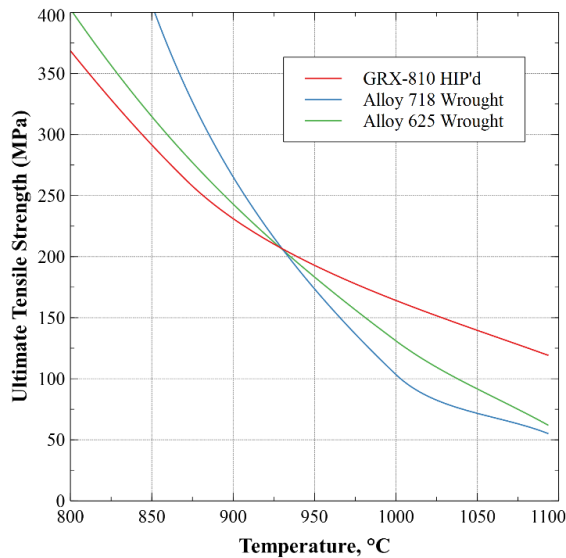


**Figure 18. Comparison of the elevated temperature tensile properties of GRX-810 compared to conventional wrought superalloys 718 and 625.**

From Figure 17, GRX-810 presents excellent tensile properties, specifically when present in extreme environments (cryogenic and high temperature). The ductility of the alloy remained above 30% at every temperature tested including cryogenic temperatures where it also exhibited high strengths. Figure 18 compares the tensile strength of GRX-810 to wrought

718 and 625. From the graph it is clear that below 900 °C the tensile properties are higher for the precipitation strengthened superalloy 718 material. However, at temperatures above 900 °C the 718 strengthening precipitates begin to overage and the grains grow, both of which significantly reduce the strength of the alloy. For GRX-810, this reduction in strength is much less pronounced due to the presence of the nano oxides throughout its microstructure. Therefore, GRX-810 presents higher strength than what was possible with non-ODS conventional superalloys. In Figure 18 GRX-810 is compared to 625 and 718 due to those alloys being amenable to the AM process and used extensively for high temperature AM components. Therefore, it is important that GRX-810 can also be printed using AM techniques. In Figure 19, images of complex geometries and components that have been built with ODS feedstock is shown.



**Figure 19. a) An oxide dispersion strengthened 3D printed combustor dome and (b) complex lattice structures.**

Figure 19 presents evidence of the printability of the coated NiCoCr family of powders and the ability to AM components that may possess better properties than what is currently possible with conventional materials and manufacturing techniques. The technology to coat and build AM ODS components is not just possible in Ni-alloys but may also be used to improve the fabrication of difficult to print refractory alloys or improve the properties of currently printed Cu and Ti – based alloys. GRX-810 represents a new class of materials that have been made possible by the arrival of AM.

## 7. Extreme Temperature Refractory Alloys

Traditional refractory metal manufacture is typically expensive due to the high feedstock cost, difficulty in forming near net shape due to fracture prone nature, as well as specialized powder production methods, heat treatment, machining, joining, surface finish enhancing, protective coating, and non-destructive evaluation (NDE) requirements [28]. Aerospace refractory metal parts tend to be thin-walled (i.e. converging-diverging nozzles) resulting in 95-98% of the stock being machined away, thus the cost of a part in feedstock alone is 5% and then 95% in machining waste, not including machining or waste disposal. Other manufacturing methods are deposition based such vacuum plasma spray, electro-deposition, etc. which tend to be relatively slow processes and require mandrels to be removed post deposition and limit part complexity. Due to the difficulty in traditional refractory metal manufacture, there are a limited number of vendors with the requisite equipment and experience [28].

AM refractory development efforts is a rapidly growing field in AM and has been conducted primarily with EB-PBF, L-PBF, binder jet, EW-DED, and LP-DED AM, showing in most cases a significant cost and schedule savings [4]. AM of C-103 is an example. Cost of an AM C-103 part has been found to be significantly less than the same part produced by conventional C-103 manufacturing, even when taking into account powder feedstock costs, print time, heat treatment, final machining, and waste disposal [29]. L-PBF and LP-DED AM C-103 is now available from a number of commercial AM suppliers to meet increasing demand. AM waste is typically 5-10% of the printed part mass resulting from over-sized powder, support structures, and sacrificial geometric features to be machined away to meet surface finish requirements.

W, Mo, Ta, Re, and various alloys of these have also been produced with AM techniques but with a wide degree of results [30]. Although printable, there is a markedly lower level of maturity due in large part to limitations in powder suppliers that can provide pre-alloyed powder that meets AM process specifications and a lack of high temperature mechanical testing that can meet relevant environmental conditions. Commercially available elemental AM grade powder options are expanded but currently limited to W, Mo, Ta, Re, and Nb; while available alloy powders include C-103, Ta3W, T5W, Ta13W. FS85 (Nb-28Ta-10W-1Zr), TZM (Mo-0.5Ti-0.08Zr-0.02C), W-25wt%Re, Mo-44wt%Re, and custom refractory high entropy alloys (RHEA) are a few still in development or

optimization for AM leveraging CALPHAD based approach.

Refractory metal components can suffer from decreased mechanical properties compared to traditional methods not only due to AM induced micro-cracking but also due to grain growth as a function of operation at elevated temperature [28]. Materials that are strengthened by fine grain AM microstructure can become ineffective at elevated temperatures as grain growth occurs. Refractory metals are known to experience this phenomenon. Carbide-dispersion strengthened (CDS) process is one of the options under development to not only address micro-cracking during the AM process but also induce grain boundary pinning to retain mechanical properties at expected operating conditions. Nano powder dispersoids can be mixed with parent metal powder prior to the AM process or can be precipitated during heat treatment, such as HfO<sub>2</sub> in AM C-103 as shown in Figure 20.

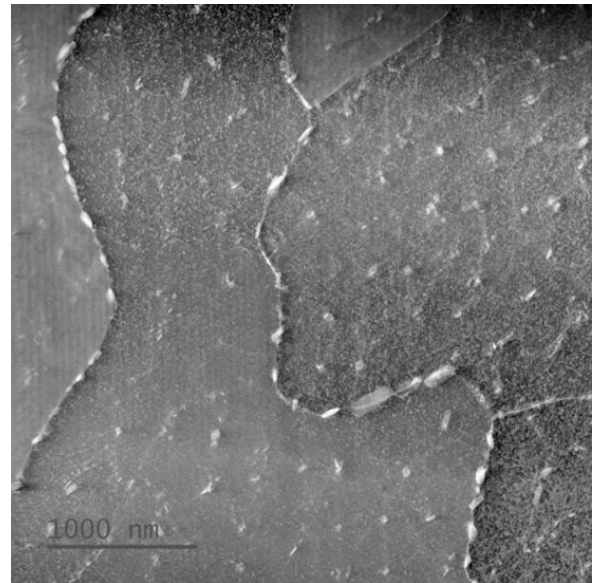


**Figure 20. Transmission electron micrograph (TEM) of L-PBF AM as-built C-103 HfO<sub>2</sub> precipitate distribution [28].**

Development of C-103 was completed using L-PBF along with vacuum stress relief at 1100 °C and HIP cycle to optimize properties of the alloy [29]. The achievable density exceeded 99.98 % TD in as built and further increased following HIP with no substantial grain growth following stress relief. Mechanical property testing of the L-PBF demonstrated the ability to achieve properties comparable and in some cases higher than wrought and meeting specification

minimums [31]. A comparison of 25 °C and 1063 °C tensile properties are shown in Figure 21.

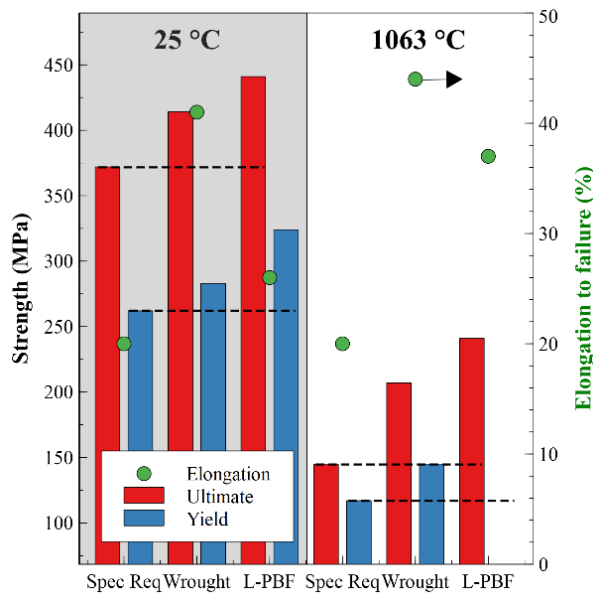


**Figure 21. Wrought vs. L-PBF C-103 ambient and elevated temperature mechanical property comparison [29].**

Additional development of pure tungsten was demonstrated using L-PBF for complex thruster components and fine lattice structures to 100  $\mu\text{m}$  strut thickness [32]. L-PBF tungsten has also been demonstrated for a simulated 1 N thruster and heated to 2300 °C successfully as shown in Figure 22.

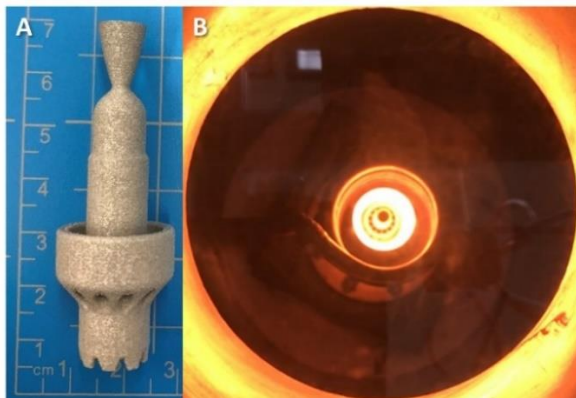


**Figure 22. A) L-PBF Tungsten 1 N green propulsion chamber, B) inductively heated to 2300 °C.**

## 8. Summary and Outlook, Future Work

Novel alloys are important to advance performance goals such as temperature and pressure capability, corrosion and wear resistance, and fatigue life in propulsion components. AM has demonstrated significant schedule and cost reduction to manufacture propulsion hardware and is being used to create complex designs as it both replaces and augments traditional manufacturing techniques. This paper emphasizes an importance of AM implementation that is intentional and systematic, at which point the designer and manufacturers can obtain the full potential of technical and economic advantages. With an in-depth understanding of various AM processes and their applicability with respect to feedstock materials, NASA has advanced many commonly available AM alloys. These AM alloys, including Copper-, Iron-, Nickel-, and refractory-based alloys, have been inserted into various propulsion applications. Novel alloys being advanced using AM include GRCo-42, GRCo-84, NASA HR-1, GRX-810, C-103, C-103 CDS, Mo, and W for specific use in rocket engines for higher performance. However, there still exists a need to develop other metallic alloys that are only possible with AM to further increase engine performance at higher operating temperatures and pressures and with longer life particularly within challenging environments such as oxygen-rich staged combustion. This paper provides a summary of the past, current, and future development work on the rocket propulsion-focused metal alloy systems. It covered the entire life cycle of AM starting from formulation, AM build processes, characterization, heat treat optimizations, microstructure characterization, mechanical and thermophysical testing, and finally ending with the engine level hot fire testing. NASA has accumulated over 100,000+ seconds and 2,200+ starts on various AM hardware including injectors, chambers, nozzles, turbomachinery, and ignition systems with many of these using the novel alloys discussed in this paper.

Activities focused on AM optimized alloys and their process development for high performance applications will continue to be prevalent in the next 10 years mainly because of the rapid technology advancement to be made in ICME. Success in these activities will not only benefit NASA but the entire AM supply chain as well as global space economy. AM has become one more tool in the manufacturing toolbox and is being accepted for fundamental rapid alloy development and production of components. While there are still many lessons learned in the

characterization of metal AM parts and alloys, the AM processes are becoming more widely adopted. In addition, the local aspect of AM, where organizations are now largely responsible for material integrity that is essential to their component production, cannot be ignored, particularly with new alloys. The immediate impact is a new emphasis on being integrated across disciplines and throughout the lifecycle of AM components and assemblies. To successfully integrate these AM alloys requires discipline to define and follow a methodical plan. Well-written standards and specification can help vastly. While the expected expansion of AM materials portfolio will certainly include proprietary materials, so there must be an appropriate IP and Trademark strategy discussion amongst stakeholders, and the awareness on sustainability commitment (i.e., reduced energy use and material waste) needs to be discussed, the outlook of AM alloy development, especially in the area of extreme environments, is very promising.

#### Acknowledgements

The authors would like to thank various partners in the development and advancement of these various alloys including RPM Innovations, Tyler Blumenthal/RPMI, Launcher Space for providing C-18150 L-PBF data (Tim Berry, Max Haot, Andre Ivankovic), AME, Elementum 3D, Castheon (ADDMan), Powder Alloy Corp, Praxair, ATI, Noah Burchett, Declan Dink Murphy, Louisiana State University (LSU) for conductivity testing, Auburn University for characterization of NASA HR-1, WMTR, IMR Testing. There are also many individuals involved in the development of these alloys across NASA and industry – thank you. Thank you to Lynn Machamer for help with graphics for formatting.

#### Appendix

**Table A: Tensile properties of HIPed GRX-810 with respect to temperature.**

Temp. (°C)	Tensile Strength (MPa)	Yield Strength (MPa)	Elong. (%)
-195.6	1227.3	723.9	49
21.1	848.1	515.0	43
426.7	655.0	410.2	40
648.9	630.9	368.9	43
871.1	262.7	206.2	62
1000.0	164.1	161.3	44
1093.3	119.3	115.8	32

#### References

- [1] Blakey-Milner B, Gradl P, Snedden G, Brooks M, Pitot J, Lopez E, et al. Metal additive manufacturing in aerospace: A review. *Mater Des* 2021;209:110008. <https://doi.org/10.1016/j.matdes.2021.110008>.
- [2] Bhat BN, editor. *Aerospace Materials and Applications*. Reston, VA: American Institute of Aeronautics and Astronautics, Inc.; 2018. <https://doi.org/10.2514/4.104893>.
- [3] Gradl, P., Tinker, D., Park, A., Mireles, O., Garcia, M., Wilkerson, R., Mckinney C. *Robust Metal Additive Manufacturing Process Selection and Development for Aerospace Components*. *J Mater Eng Performance*, Springer 2021. <https://doi.org/10.1007/s11665-022-06850-0>.
- [4] Paul R. Gradl, Omar R. Mireles, Christopher S. Protz, Chance P. Garcia. *Metal Additive Manufacturing for Propulsion Applications*. 1st ed. Reston, VA: American Institute of Aeronautics and Astronautics, Inc.; 2022. <https://doi.org/10.2514/4.106279>.
- [5] Gradl PR, Greene SE, Protz C, Bullard B, Buzzell J, Garcia C, et al. Additive manufacturing of liquid rocket engine combustion devices: A summary of process developments and hot-fire testing results. 2018 *Jt. Propuls. Conf.*, American Institute of Aeronautics and Astronautics Inc, AIAA; 2018. <https://doi.org/10.2514/6.2018-4625>.
- [6] Gradl PR, Protz CS, Ellis DL, Greene SE. Progress in additively manufactured copper-alloy GRCop-84, GRCop-42, and bimetallic combustion chambers for liquid rocket engines. *Proc. Int. Astronaut. Congr. IAC 2019*, vol. October 21, 2019, p. 21–5.
- [7] Gradl PR, Protz CS. Technology advancements for channel wall nozzle manufacturing in liquid rocket engines. *Acta Astronaut* 2020;174. <https://doi.org/10.1016/j.actaastro.2020.04.067>
- [8] Smith TM, Thompson AC, Gabb TP, Bowman CL, Kantzos CA. Efficient production of a high-performance dispersion strengthened, multi-principal element alloy. *Sci Reports* 2020 101 2020;10:1–9. <https://doi.org/10.1038/s41598-020-66436-5>.
- [9] National Research Council (U.S.). Committee on Integrated Computational Materials Engineering. *Integrated computational materials engineering : a transformational discipline for improved competitiveness and national security*

- 2008:137.
- [10] Seifi M, Salem A, Beuth J, Harrysson O, Lewandowski JJ. Overview of Materials Qualification Needs for Metal Additive Manufacturing. *JOM* 2016;68:747–64. <https://doi.org/10.1007/s11837-015-1810-0>.
- [11] Song Q song, Zhang Y, Wei Y feng, Zhou X yi, Shen Y fu, Zhou Y min, et al. Microstructure and mechanical performance of ODS superalloys manufactured by selective laser melting. *Opt Laser Technol* 2021;144:107423. <https://doi.org/10.1016/J.OPTLASTEC.2021.107423>.
- [12] Kerstens F, Cervone A, Gradl P. End to end process evaluation for additively manufactured liquid rocket engine thrust chambers. *Acta Astronaut* 2021;182:454–65. <https://doi.org/10.1016/j.actaastro.2021.02.034>
- [13] Minneci RP, Lass EA, Bunn JR, Choo H, Rawl CJ. Copper-based alloys for structural high-heat-flux applications: a review of development, properties, and performance of Cu-rich Cu–Cr–Nb alloys. *Int Mater Rev* 2020. <https://doi.org/10.1080/09506608.2020.1821485>
- [14] Lee J. Hydrogen embrittlement. 2016.
- [15] Li M, Zinkle SJ. Physical and Mechanical Properties of Copper and Copper Alloys. *Compr Nucl Mater* 2012;4:667–90. <https://doi.org/10.1016/B978-0-08-056033-5.00122-1>.
- [16] De Groh HC, Ellis DL, Loewenthal WS. Comparison of GRCo-84 to Other Cu Alloys With High Thermal Conductivities n.d.
- [17] Gradl PR, Protz C, Cooper K, Garcia C, Ellis D, Evans L. GRCo-42 development and hot-fire testing using additive manufacturing powder bed fusion for channel-cooled combustion chambers. *AIAA Propuls. Energy Forum Expo*. 2019, American Institute of Aeronautics and Astronautics Inc, AIAA; 2019. <https://doi.org/10.2514/6.2019-4228>.
- [18] Wadsworth J, Nieh TG, Stephens JJ. Recent advances in aerospace refractory metal alloys. [Http://DxDoiOrg/101179/Imr1988331131](http://DxDoiOrg/101179/Imr1988331131) 2013;33:131–50. <https://doi.org/10.1179/IMR.1988.33.1.131>.
- [19] Katsarelis C, Chen P, Gradl PR, Protz C, Jones Z, Marshall N, et al. Additive Manufacturing of NASA HR-1 Material for Liquid Rocket Engine Component Applications. *JANNAF Jt Propuls Conf* 2019;<https://ntrs.nasa.gov/search.jsp?R=20200001007>.
- [20] Chen PS, Katsarelis CC, Medders WM, Gradl PR. Segregation Evolution and Diffusion of Titanium in Directed Energy Deposited. 2021.
- [21] Gradl PR, Teasley TW, Protz CS, Katsarelis C, Chen P. Process Development and Hot-fire Testing of Additively Manufactured NASA HR-1 for Liquid Rocket Engine Applications. *AIAA Propuls. Energy* 2021, 2021, p. 1–23. <https://doi.org/10.2514/6.2021-3236>.
- [22] Chen P-S, Mitchell M. *Aerospace Structural Metals Handbook ALLOY NASA-HR-1 Nickel Base Alloys-Ni*. 2005.
- [23] Brif Y, Thomas M, Todd I. The use of high-entropy alloys in additive manufacturing. *Scri Mater* 2015;99:93–6. <https://doi.org/10.1016/j.scriptamat.2014.11.037>
- [24] Chen S, Tong Y, Liaw PK. Additive manufacturing of high-entropy alloys: A review. *Entropy* 2018;20. <https://doi.org/10.3390/e20120937>.
- [25] Weng F, Chew Y, Zhu Z, Yao X, Wang L, Ng FL, et al. Excellent combination of strength and ductility of CoCrNi medium entropy alloy fabricated by laser aided additive manufacturing. *Addit Manuf* 2020;34:101202. <https://doi.org/10.1016/j.addma.2020.101202>.
- [26] Smith TM, Thompson AC, Gabb TP, Bowman CL, Kantzos CA. Efficient production of a high-performance dispersion element alloy. *Sci Rep* 2020;1–9. <https://doi.org/10.1038/s41598-020-66436-5>.
- [27] Smith TM. Additive Manufactured Alloys for High Temperature Applications. *NASA T2 Webinar* 2022.
- [28] Mireles O. Additive Manufacture of Refractory Metals for Aerospace Applications. *AIAA Propuls. Energy* 2020 Forum, 2021, p. 1–9. <https://doi.org/10.2514/6.2021-3234>.
- [29] Mireles OR, Rodriguez O, Gao Y, Philips N. Additive manufacture of refractory alloy C-103 for propulsion applications. *AIAA Propuls. Energy* 2020 Forum, American Institute of Aeronautics and Astronautics Inc, AIAA; 2020, p. 1–13. <https://doi.org/10.2514/6.2020-3500>.
- [30] Talignani A, Seede R, Whitt A, Zheng S, Ye J, Karaman I, et al. A review on additive manufacturing of refractory tungsten and tungsten alloys. *Addit Manuf* 2022;58:103009. <https://doi.org/10.1016/J.ADDMA.2022.103009>
- [31] Awasthi PD, Agrawal P, Haridas RS, Mishra RS, Stawovy MT, Ohm S, et al. Mechanical properties and microstructural characteristics of additively manufactured C-103 niobium alloy.

Mater Sci Eng A 2022;831:142183.  
<https://doi.org/10.1016/J.MSEA.2021.142183>.

- [32] Romnes CJ, Stubbins JF, Mireles OR. Tuning the Properties of Additively Manufactured Tungsten Ultra-fine Lattices by Adjusting Laser Energy Density and Lattice Geometry. J Mater Eng Perform 2022 2022:1–14.  
<https://doi.org/10.1007/S11665-022-07126-3>.